Helical Multicore Fiber-Based Vibration Sensing

Danxia Lu, Xing Rao, Shangwei Dai, Shen Liu, Guo-Wei Lu, *Member, IEEE*, Yiping Wang, *Senior Member, IEEE*, and George Y. Chen, *Senior Member, IEEE*

***Abstract*—Long-distance monitoring of vibrations is essential for smart infrastructure. Forward transmissions distributed sensing technologies lead the way in sensing distance, albeit with an extra layer of complexity caused by synchronization for vibration positioning. A unidirectional distributed fiber-optic vibration sensing system using helical multicore fiber (HMCF) is proposed and demonstrated to overcome the synchronization challenge. By exploiting the optical path difference between straight and helical cores in a single optical fiber, and employing self-referencing interferometric in-phase/quadrature (IQ) demodulation, distributed vibration positioning can be achieved without bidirectional transmission, long-distance detector synchronization, multiple wavelength channels, or backscatter noise suppression. The proof-of-concept experimental results reveal a minimum standard positioning deviation of 28 m over 20 km of sensing fiber. The sensitivities of the straight core and helical core are 8.6 and 9.1 rad/$\mu\varepsilon$, respectively, with the helical structure enhancing sensitivity by 5.5%. The corresponding limit of detection (LoD) is 26.4 and 22.6 pε/Hz$^{1/2}$. The combination of space-division multiplexing (SDM) and forward transmission methods can open up a new avenue for fully distributed sensing.**

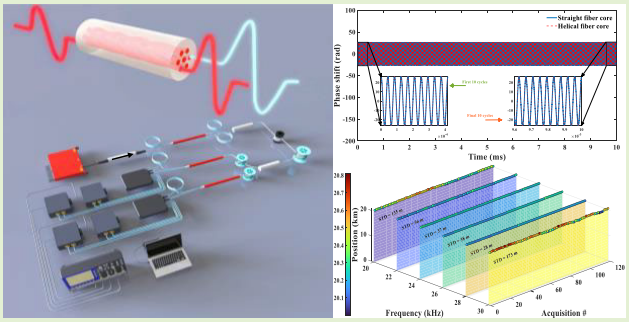

***Index Terms*—Forward transmission, distributed fiber-optic sensor, forward DAS, helical multicore fiber (HMCF), vibration sensor.**

I. Introduction

DISTRIBUTED fiber-optic vibration sensors utilize light waves as the carrier and optical fiber as the sensing and transmission medium. They enable large-scale, real-time monitoring of external disturbances, and are indispensable in fields such as structural health monitoring [1], [2], border security [3], and oil/gas pipeline leak detection [4]. However, conventional approaches mostly rely on backscattering mechanisms (e.g., Rayleigh scattering-based Φ-OTDR [5]), which suffer from significant inherent limitations: 1) weak backscattered signal strength and round-trip transmission losses; 2) dependence on pulsed sources that limit high-frequency response due to pulse repetition rates, making it difficult to capture rapid disturbances above several kilohertz; and 3) additional noise introduced by random process of Rayleigh scattering, which can easily overwhelm the signal over long distances, failing to meet the demands of ultralong-range, high-sensitivity monitoring.

In recent years, forward transmission-based distributed sensing schemes have achieved remarkable progress [6], [7], [8]. Forward transmission, which does not rely on backscattering mechanisms, typically utilizes continuous-wave (CW) light propagating along the fiber, fundamentally addressing the issues of weak signal strength and/or short sensing distance. As a result, unidirectional forward transmission architectures have demonstrated distinct advantages. For example, Chen et al. [9] employed a single unidirectional Mach–Zehnder interferometer (MZI), leveraging dispersion-induced walk-off to locate vibration events, and achieved a sensing distance of 320 km by incorporating multistage

Received 14 November 2025; revised 19 January 2026; accepted 22 January 2026. Date of publication 3 February 2026; date of current version 16 March 2026. This work was supported in part by the National Natural Science Foundation of China under Grant 62275172, Grant U22A2088, and Grant W2532046; in part by Shenzhen Science and Technology Program (Shenzhen Key Laboratory of Ultrafast Laser Micro/Nano Manufacturing) under Grant ZDSYS20220606100405013; in part by Shenzhen Science and Technology Program under Grant JCYJ20241202124408012 and Grant JCYJ20220818095800001; in part by the Scientific Instrument Developing Program of Shenzhen University under Grant 2023YQ027; and in part by the Research Team Cultivation Program of Shenzhen University under Grant 2023DFT001. The associate editor coordinating the review of this article and approving it for publication was Dr. Ginu Rajan. *(Corresponding author: George Y. Chen.)*

Danxia Lu, Xing Rao, Shangwei Dai, Shen Liu, Yiping Wang, and George Y. Chen are with the State Key Laboratory of Radio Frequency Heterogeneous Integration, Key Laboratory of Optoelectronic Devices and Systems of Ministry of Education and Guangdong Province, College of Physics and Optoelectronic Engineering, and Shenzhen Key Laboratory of Ultrafast Laser Micro/Nano Manufacturing, Guangdong and Hong Kong Joint Research Center for Optical Fiber Sensors, Shenzhen University, Shenzhen, Guangdong 518060, China (e-mail: 2300453040@email.szu.edu.cn; 2250453012@email.szu.edu.cn; daishangwei2023@email.szu.edu.cn; shenliu@szu.edu.cn; ypwang@szu.edu.cn; gychen@szu.edu.cn).

Guo-Wei Lu is with the Institute for Materials Chemistry and Engineering, Kyushu University, Fukuoka 816-8580, Japan (e-mail: gordon.guoweilu@gmail.com).

Digital Object Identifier 10.1109/JSEN.2026.3658041

EDFA amplification. Huang et al. [10] proposed a dual-Sagnac interferometer configuration with a polarization compensation module to mitigate polarization instability, achieving 150-km coverage without repeaters and a positioning error (depending on calibration) within ±30 m through time-delay estimation algorithms. Yan et al. [11] developed a system combining forward transmission with coherent detection and frequency-shifted time-delay lines, realizing a 615-km sensing range over a 1230-km fiber link, with a spatial resolution better than 125 m for vibrations above 1 kHz. In addition, a loop-back structure based on unidirectional forward transmission achieved a positioning accuracy of ±100 m for single point and ±200 m for multipoint vibrations over 500 km [12].

Multicore fibers (MCFs), as key photonic devices for overcoming the limitations of conventional single fiber sensing, are designed to integrate multiple independent cores within a single fiber, enabling space-division multiplexing (SDM) and significantly enhancing communication system capacity and throughput [13]. Their spatially separated core structure provides a foundation for overcoming Rayleigh backscattering interference in cofiber configurations. Zhao et al. [14] implemented a spatial-division multiplexed MZI using a seven-core fiber, successfully eliminating coherent Rayleigh scattering interference. Through single-wavelength illumination and cross-correlational processing, the system achieved 54.9-m root-mean-squared error (RMSE) over 38.5 km, validating MCFs' capability for constructing differentiated, interference-resistant sensing paths.

Over the past decade, research on helical MCF (HMCF) and their use in fiber-optic sensing has seen significant advances. Their distinct helical geometry induces circular birefringence, enhances mechanical sensitivity, and enables controllable path length engineering, making them widely applicable in various types of sensors. Possible measurands include torsion [15], [16], strain [17], bending [18], temperature [19], refractive index [20], magnetic field [21], and current [22]. However, despite the broad range of sensing applications, leveraging the inherent optical path difference of HMCF specifically for forward transmission distributed sensing and positioning has not been reported in the literature. Moreover, conventional MCF-based sensing systems often rely on loop-back architectures to facilitate signal return for interference, posing challenges in practical deployment, including structural complexity and incompatibility with integrated communication and sensing (ISAC) systems. The unidirectional architecture proposed in this work allows for compatibility with ISAC systems, flexible allocation of cores for communication and sensing, and signal separation in the frequency domain.

In this work, we propose the effective use of HMCF for realizing unidirectional forward transmission distributed sensing, and demonstrate its ability in performing vibration measurements. This sensing system employs free-space coupling optics to launch a CW laser into the straight and helical cores of the HMCF, forming two distinct forward-propagating channels with different optical path lengths. Due to periodic winding along the axis of the helical core, its actual optical path length is inherently longer than that of the straight core. This intrinsic path length difference serves as the basis for vibration positioning, eliminating the need for bidirectional transmission, long-distance detector synchronization, and multiple wavelength channels. Moreover, it avoids the signal-to-noise ratio (SNR) degradation and coherent interference associated with backscatter noise. In addition, two independent self-referencing interferometric in-phase/quadrature (IQ) [24], [25] detection modules are employed to demodulate the phase information from the two forward-propagating signals while effectively suppressing common-mode noise. Both IQ demodulation channels are sampled by the same oscilloscope, ensuring inherent synchronization. As the system architecture relies on a single wavelength, unidirectional transmission, and spatial-division multiplexing, it minimizes positioning distortions caused by dispersion and group delay differences typical of multiwavelength systems, which makes it suitable for long-distance vibration positioning.

II. Operating Principles

When an external vibration occurs at a certain position along the fiber-under-test (FUT), the local refractive index and fiber birefringence are dynamically modified due to the photoelastic effect and physical deformation, resulting in-phase modulation of the forward-propagating optical signal. Physical deformation of the sensing fiber can be classified as axial strain or bending. Axial strain involves path length change as well as the photoelastic effect that modifies the effective index. On the other hand, bending induces linear birefringence. The overall phase delay is determined by the path length and effective index, as well as the linear birefringence that could add or subtract phase delay depending on the alignment between the polarized light and the birefringent axes. To investigate the phase response characteristics of the system under vibration (i.e., dynamic strain), the HMCF is wound around a disk-shaped piezoelectric transducer (PZT), which is driven by a periodic sinusoidal voltage signal generated by an arbitrary waveform generator to simulate external disturbances.

Assuming that a disturbance signal is applied to the helical fiber, the modulated optical signal is mixed with a time-delayed reference signal at the detection end. At the output of the BPD, the resulting interferometric signal is separated into in-phase (I) and quadrature (Q) components, which can be expressed as

$$I(t) = I_0 \cos\left(k_0 c \Delta\tau + \varphi(t) - \varphi(t - \Delta\tau)\right) \tag{1}$$

$$Q(t) = I_0 \sin\left(k_0 c \Delta\tau + \varphi(t) - \varphi(t - \Delta\tau)\right) \tag{2}$$

where I_0 denotes the interference intensity between the reference path and its time-delayed path, k_0 is the wavenumber, c is the speed of light in vacuum, $\Delta\tau$ represents the fixed time delay introduced by the delay fiber, $\varphi(t)$ is the phase signal induced by the vibration, and $\varphi(t - \Delta\tau)$ denotes the phase-modulated signal passing through the delay fiber.

Since the coherent IQ detection technique enables full optical field retrieval, the phase information carrying the disturbance can be extracted from the signal and expressed as

$$\Delta\varphi(t) = \varphi(t) - \varphi(t - \Delta\tau). \tag{3}$$

If the vibration affects the sensing fiber at a sensing distance L from the detection end, the corresponding transmission length along the straight core is denoted as L_H. $L_H = 1.001 \times L$ can be used to represent the path length of the helical core, according to the manufacturer's specifications (84 μm in diameter and 6 mm in helix pitch). Given that the time-delay fiber has length L_d, the time delay introduced is $L_d = \Delta\tau \times n/c$, where n is the effective refractive index of the fiber core. The propagation time for the probe light traveling from the vibration positioning to the hybrid via the straight-core path is given by $t_1 = L \times n/c$, and via the helical-core sensing path is $t_2 = L_H \times n/c$.

The demodulated phase signal from the straight-core sensing path is denoted as $\Delta\varphi_1(t)$, which can be expressed as

$$\Delta\varphi_1(t) = \varphi(t - t_1) - \varphi(t - t_1 - \Delta\tau). \tag{4}$$

Similarly, the demodulated phase signal from the helical-core sensing path is denoted as $\Delta\varphi_2(t)$, which can be expressed as

$$\Delta\varphi_2(t) = \varphi(t - t_2) - \varphi(t - t_2 - \Delta\tau). \tag{5}$$

Assuming that Δt is the time delay between the time-of-arrival of the vibration-induced phase signals at the detection modules, Δt can be expressed as

$$\Delta t = t_2 - t_1 = \frac{L_H \times n}{c} - \frac{L \times n}{c} = \frac{0.001nL}{c}. \tag{6}$$

Thus, the vibration position L can be determined by the following equation:

$$L = \frac{c\Delta t}{0.001n} \tag{7}$$

where Δt can be determined by applying a phase-spectrum-based time-delay estimation algorithm [25] to the copropagating phase-modulated signals, $\Delta\varphi_1(t)$ and $\Delta\varphi_2(t)$.

The phase-spectrum-based time-delay estimation principles and implementations are as follows. The phase signals demodulated from the straight- and helical-core paths, $\Delta\varphi_1(t)$ and $\Delta\varphi_2(t)$, are related by a vibration position-dependent time-delay Δt such that $\Delta\varphi_2(t) \approx \Delta\varphi_1(t + \Delta t)$. The Fourier transforms of these signals yield their phase spectra, $\varphi_1(f)$ and $\varphi_2(f)$. Leveraging the time-shift property of the Fourier transform, the difference between the pair of phase spectra is linear with respect to frequency within the signal band

$$\varphi_2(f) - \varphi_1(f) = 2\pi f \Delta t. \tag{8}$$

Thus, the time-delay Δt_f at each frequency component f can be directly calculated by

$$\Delta t_f = \frac{\varphi_2(f) - \varphi_1(f)}{2\pi f}. \tag{9}$$

The vibration location L is then obtained by substituting the calculated Δt_f into (7). This method offers a key advantage over conventional time-domain cross correlation. By operating in the frequency domain, it can effectively separate multiple vibration components of different frequencies that are mixed in the time-domain signal and compute a distinct time delay for each frequency component. This method is the foundation for multipoint vibration positioning.

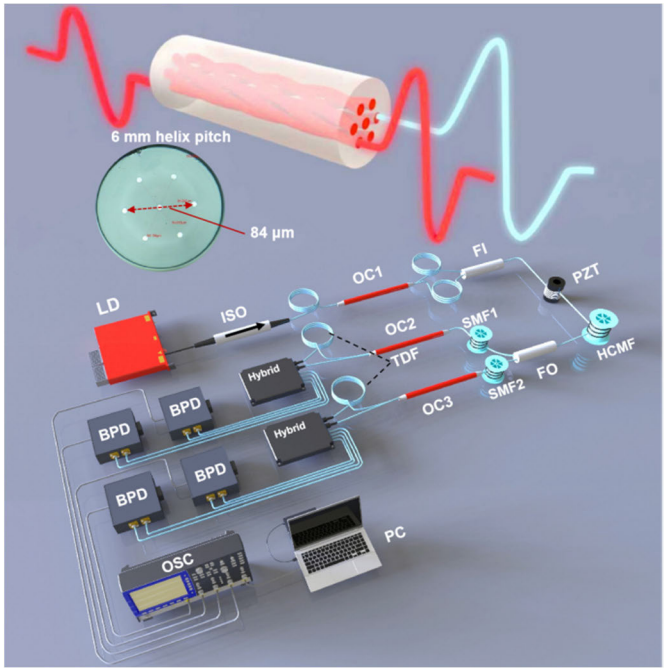

Fig. 1. Schematic of the unidirectional distributed sensing system. LD: laser diode; ISO: isolator; OC1, OC2, and OC3: optical couplers; PZT: piezoelectric transducer; FI/FO: fan-in/fan-out device; HCMF: helical multicore fiber; SMF1 and SMF2: single-mode fibers 1 and 2; TDF: time-delay fiber; Hybrid: 90° optical hybrid; BPD: balanced photodetector; OSC: oscilloscope; and PC: personal computer. Inset: cross-sectional structure of the helical multicore.

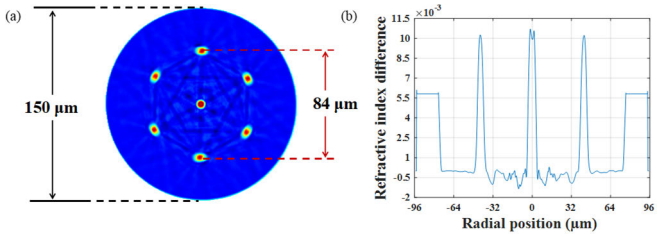

Fig. 2. Structural and optical characteristics of HMCF. (a) Mode field distribution. (b) Refractive index profile.

III. Experimental Design

To verify the feasibility of the proposed vibration sensing scheme, the unidirectional forward transmission sensing system based on HMCF was established, as illustrated in Fig. 1.

A narrow-linewidth (<100 Hz) laser (Koheras BASIK E15, NKT Photonics) is used as the light source. Its output was split into two via a 50:50 fiber coupler. These two optical beams are coupled into the straight core and helical core of the HMCF via a fan-in (FI) device, which, together with the fan-out (FO) device, exhibits an insertion loss of <1 dB and an intercore crosstalk of approximately −60 dB, ensuring efficient and independent excitation of the two sensing cores. The employed HMCF features a central straight core and six outer helical cores that revolves around the central core with a rotational diameter of 84 μm and a helix pitch of 6 mm. The mode field distribution and refractive index profile of the HMCF are shown in Fig. 2(a) and (b), respectively. Fig. 2(a) confirms the single-mode guidance condition for all cores. Fig. 2(b)

demonstrates that the central straight core and the surrounding helical cores exhibit nearly identical refractive index contrasts, indicating matched waveguide structures between the straight and helical cores, which is a critical prerequisite for stable interference and consistent group delay characteristics in our sensing scheme. The length of HCMF is approximately 80 m. At the far end of the HMCF, light from the straight core and helical core is coupled into two single-mode fibers (SMFs) via an FO device. Here, the SMF connected to the straight core is approximately 20 km long, where the length ratio of the two SMFs matches the path length ratio within the HMCF (extension for demonstration), making the total fiber length 20.23 km from the source to the demodulator for the HMCF path. This SMF extension is for amplifying the optical path difference and thus time delay of the HMCF, thereby validating the positioning method under a realistic long-distance deployment, and then split by a coupler for self-referencing interferometric demodulation (lower requirement on laser coherence). The coherence length of the laser only needs to exceed the optical path difference introduced by the delay fiber. Standard IQ phase demodulation is performed using a 100-m delay fiber and a 90° optical hybrid (Hybrid). Subsequently, the orthogonal optical intensity signals output from the two Hybrids are received by pairs of BPDs (Thorlabs PDB470C-AC, 400-MHz bandwidth), converted into electrical signals, and fed into a real-time oscilloscope (1-GHz bandwidth). The phase information is then extracted through digital signal processing algorithms to determine the position and strength of the disturbance events.

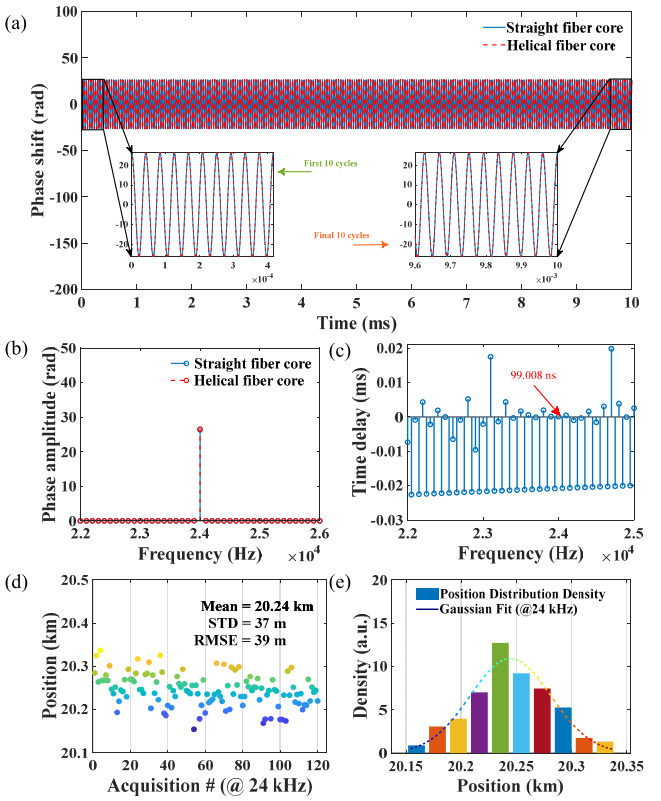

Fig. 3. Single-point vibration measurements. (a) Demodulated time-domain waveform. (b) FFT of the phase signal from the straight fiber core and helical fiber core. (c) Time-delay spectrum between $\Delta\varphi_1(t)$ and $\Delta\varphi_2(t)$. (d) Positioning results based on 120 datasets. (e) Histogram of the distribution of calculated vibration positions.

IV. Experimental Results

A. Single-Point Vibration Measurements

To experimentally validate the positioning mechanism, a PZT wrapped with 5 m of SMF was first placed before OC1, with the sensing fiber length L being 20.23 km. In the following experiment, the PZT was driven by a sinusoidal signal of 24-kHz and 60-V amplitudes, generated by an arbitrary waveform generator. To remove the dc component and resolve phase ambiguity, normalization is applied first, followed by the arctangent operation and then phase unwrap. Fig. 3(a) displays the demodulated phase signals from the two IQ detection modules. Over a 10-ms time window, the recovered vibration signals vary periodically, with the inset showing a zoomed-in view of the first and last ten cycles of the vibration signal. Fig. 3(b) presents the amplitude spectrum, where a prominent peak at 24 kHz indicates successful detection of the phase modulation induced by the vibration. Using the phase-spectrum time-delay method, a time delay of 99.008 ns between two phase signals is obtained, as shown in Fig. 3(c). With a fiber refractive index n = 1.467, the corresponding vibration position can be calculated as 20.25 km.

In order to quantify the system's positioning reliability, repeated vibration experiments were conducted to investigate its positioning accuracy. The positioning results (L) obtained from 120 successive positioning are shown in Fig. 3(d), and the corresponding histogram of the statistical distribution is presented in Fig. 3(e). The Gaussian fitting analysis reveals that the peak of the probability distribution is located at 20.24 km, which is in excellent agreement with the actual vibration position. Based on all the measurement data, the standard deviation (STD) and RMSE of the positioning results are calculated to be 37 and 39 m, respectively.

The frequency response of the system was subsequently characterized, with the signal frequency swept from 20 to 30 kHz in 2-kHz steps. The disturbance events were positioned by analyzing the acquired phase signals using the phase–time-delay spectrum method. To enhance the reliability of the experimental data, 120 measurements were performed at each vibration frequency, with each measurement sampled at 312.5 MS/s over a 10-ms window, resulting in 3.125-M samples per dataset. The maximum value of the STD for the positioning results is 173 m, and the minimum value is 28 m, indicating that the positioning accuracy varies across the frequency spectrum. This discrepancy arises from frequency-dependent system characteristics, as well as minor environmental disturbances such as temperature drifts or stray mechanical stress during the experiments. More specifically, such frequency-dependent fluctuation is a common characteristic found in many interferometric systems relying on time-delay estimation (e.g., dual-Michelson or dual-MZI configurations). The significant increase in RMSE or STD, particularly near 30 kHz, is primarily attributed to the frequency-dependent response of the PZT used to simulate the vibration. As the driving frequency approaches the mechanical resonance of the PZT, its vibration behavior becomes unstable

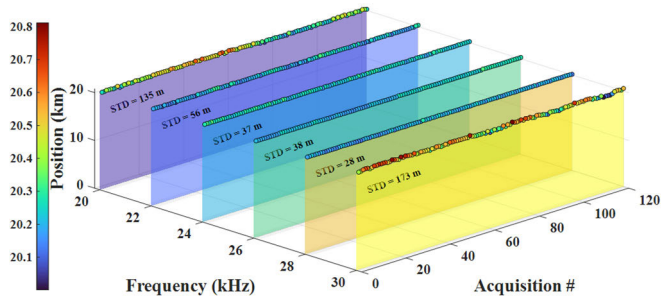

Fig. 4. Positioning accuracy statistics under different vibration frequencies.

and nonlinear. Crucially, the self-referencing interferometric IQ demodulation used for two cores is sensitive to a reduction in the SNR. The diminished phase modulation amplitude from the PZT on the resonance directly leads to a lower SNR, which in turn disproportionately degrades the precision of the time-delay estimation. This highlights a limitation of the current experimental setup rather than the fundamental positioning principle. It is worth noting that the system performance could be further improved by optimizing the length of the delay fiber. As shown in Fig. 4, the positioning performances under different vibration frequencies demonstrate fair consistency and repeatability across the tested frequency range.

To evaluate the vibration sensitivity of the two sensing paths in the HMCF, dynamic strain experiments were conducted using a PZT. In the experiment, approximately 2.5 m of HMCF were uniformly wound on a PZT of approximately 50 mm in diameter to apply a controlled cyclic strain and placed at the beginning of the sensing fiber. It should be noted that the amplitude of the phase signal is heavily influenced by the time delay induced by the TDF and the vibration frequency. Given the limited displacement responsivity of the PZT, and to ensure that the fiber delay length remains within the coherence length of the laser source, the TDF was extended to 1 km from 100 m to enhance the overall phase response of the system. A sinusoidal signal at 20 kHz with a driving voltage ranging from 0 to 60 V was applied to the PZT. Demodulated phase signals with different amplitudes are presented in Fig. 5, each segment having a time duration of 1 ms. The fast Fourier transform (FFT) was performed on the demodulated phase signals to extract the amplitude at the excitation frequency. For each voltage level, ten sets of data were collected to calculate the average phase amplitude. As illustrated in Fig. 5(b) and (c), linear fitting of the phase response under different strain levels yielded the sensitivities of the two independent sensing paths—straight core and helical core. The results show that the sensitivity is 8.6315 rad/$\mu\varepsilon$ for the straight core and 9.1298 rad/$\mu\varepsilon$ for the helical core. Due to the helical geometry, which involves longer path length and direction-dependent strain coupling, the helical core exhibits a slightly higher sensitivity to mechanical deformation induced by external perturbations, showing an enhancement of approximately 5.46% compared to the straight core under identical conditions.

In order to understand how the positioning accuracy is affected after moving the position of the PZT (after FI)

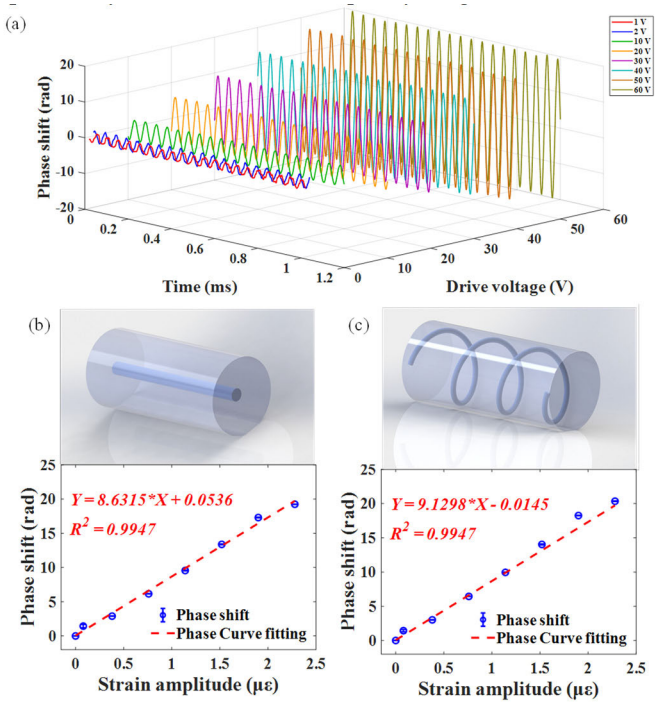

Fig. 5. Phase response and sensitivity (at 20 kHz). (a) Phase demodulation results under different vibration amplitudes. Phase sensitivity for (b) straight-core sensing path and (c) helical-core sensing path.

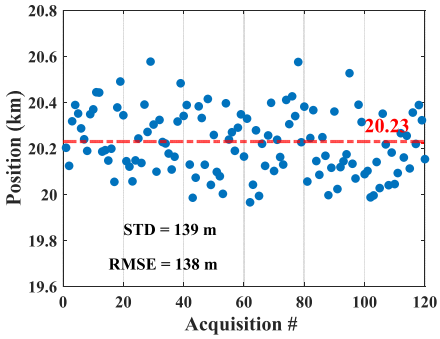

Fig. 6. Consecutive vibration positioning measurements under a 40-kHz sinusoidal signal.

from a section of SMF to HMCF, 120 datasets of 40-kHz high-frequency sinusoidal vibration signal were continuously acquired and analyzed, with the acquisition time of a single sample being 10 ms, and the sampling rate being set to 312.5 MS/s. The RMSE was calculated with respect to the true vibration position as a metric of the positioning accuracy. The experimentally measured RMSE of the system is 138 m, as shown in Fig. 6.

To assess the limit of detection (LoD) of the sensing system, phase noise was recorded over a duration of 10 ms in the absence of external vibrations. The STD of the noise was calculated to determine the noise floor. The measured phase noise STD is 1.382 and 1.251 rad for the straight core and helical core, respectively. The LoD (LoD = 3.3 × std (phase noise)/sensitivity) is deduced as 0.528 $\mu\varepsilon$ for the straight core and 0.452 $\mu\varepsilon$ for the helical core. Considering the 400-MHz bandwidth of BPDs, the normalized LoD can be obtained

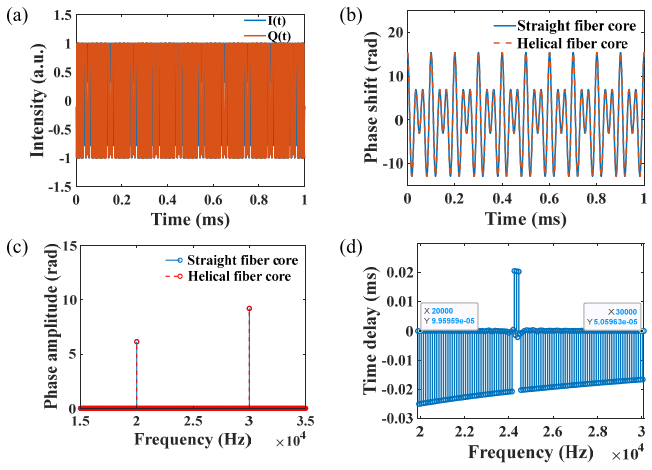

Fig. 7. Multipoint vibration simulation. (a) In-phase and quadrature interferometric signals are output from the optical hybrids. (b) Demodulated phase signals for the two vibration points. (c) Amplitude–frequency spectrum obtained via FFT. (d) Time-delay spectrum.

by dividing the LoD by the square root of the detection bandwidth, resulting in 26.4 and 22.6 $p\varepsilon/Hz^{1/2}$ for the straight core and helical core, respectively.

B. Multipoint Vibration Simulation

Due to the difficulty of implementing multivibration-source excitation in the experiments with limited HMCF resources, the multipoint positioning capability was demonstrated through numerical simulation. It should be noted that previous works involving multipoint vibration measurements were successfully demonstrated using the phase-spectrum time-delay method [12], [25]. In the simulation, high-frequency vibration signals at 20 and 30 kHz were simultaneously applied at positions of 20 and 10 km from the detection end, respectively. The spatial resolution of the proposed phase-spectrum method can be described by $\delta z = c/(2nNf)$, where c is the speed of light in vacuum, $n \approx 1.467$ is the effective refractive index of the fiber, $N = 3.125$ M is the total number of samples per dataset, and f is the vibration frequency. Under these conditions, the theoretical spatial resolution is of the order of millimeters. Fig. 7(a) shows the in-phase (I) and quadrature (Q) interferometric intensity signals output from the optical hybrid. The demodulated phase–time traces are plotted in Fig. 7(b). A frequency spectrum analysis of the demodulated signals yields the amplitude–frequency spectrum shown in Fig. 7(c), where distinct peaks appear at 20 and 30 kHz, indicating excellent frequency resolution. Using the phase-spectrum time-delay method, the time delay between spatial channels corresponding to each frequency component can be calculated. As shown in Fig. 7(d), the time delays are 99.596 and 50.596 ns. Based on the time-delay-to-distance mapping relationship, the corresponding vibration positions are retrieved as 20.367 and 10.347 km.

V. Conclusion

This proof-of-concept study demonstrates the feasibility of a unidirectional, forward transmission-based distributed vibration sensing scheme using HMCF. Unlike conventional approaches relying on backscattering or bidirectional transmission configuration, the proposed system employs unidirectional phase demodulation and SDM-based positioning by exploiting the optical path length difference between the helical core and the straight core. The system architecture is elegant and avoids the need for complex detector synchronization. The experimental results show that the sensing system can achieve a minimum standard positioning deviation of 28 m over a sensing distance of 20 km, with good repeatability maintained across the 20–30-kHz ultrasonic frequency range. The vibration-to-phase sensitivities of the straight- and helical-core sensing paths are 8.6315 and 9.1298 rad/$\mu\varepsilon$ at 20 kHz, respectively, corresponding to an LoD of 26.4 and 22.6 $p\varepsilon/Hz^{1/2}$. The helical core exhibits a 5.46% higher sensitivity to external vibrations compared to the straight core. The demonstrated sensing system is applicable to a range of applications requiring nonfiber-loop distributed sensing and/or high-frequency response, such as national rail and partial discharge monitoring.

References

[1] J. M. Lopez-Higuera, L. Rodriguez Cobo, A. Quintela Incera, and A. Cobo, "Fiber optic sensors in structural health monitoring," *J. Lightw. Technol.*, vol. 29, no. 4, pp. 587–608, Feb. 15, 2011.

[2] K. Bremer, F. Weigand, Y. Zheng, L. Alwis, R. Helbig, and B. Roth, "Structural health monitoring using textile reinforcement structures with integrated optical fiber sensors," *Sensors*, vol. 17, no. 2, p. 345, Feb. 2017.

[3] X. Li, Q. Sun, J. Wo, M. Zhang, and D. Liu, "Hybrid TDM/WDM-based fiber-optic sensor network for perimeter intrusion detection," *J. Lightw. Technol.*, vol. 30, no. 8, pp. 1113–1119, Apr. 15, 2012.

[4] Y. Huang, Q. Wang, L. Shi, and Q. Yang, "Underwater gas pipeline leakage source localization by distributed fiber-optic sensing based on particle swarm optimization tuning of the support vector machine," *Appl. Opt.*, vol. 55, no. 2, pp. 242–247, Jan. 2016.

[5] X. Bao, D.-P. Zhou, C. Baker, and L. Chen, "Recent development in the distributed fiber optic acoustic and ultrasonic detection," *J. Lightw. Technol.*, vol. 35, no. 16, pp. 3256–3267, Aug. 15, 2017.

[6] Z. Sun, D. Huang, S. Li, H. Yang, and C. Zhao, "High-efficiency positioning of vibration intrusions for long-distance perimeter security monitoring based on time-frequency variation envelopes," *IEEE Trans. Instrum. Meas.*, vol. 73, pp. 1–11, 2024.

[7] Z. Wu, Z. Wu, and A. Sun, "Long distance distributed optical fiber vibration sensing and positioning technology based on loop transmission polarization detection," *Measurement*, vol. 225, Feb. 2024, Art. no. 114029.

[8] F. Shi, R. Jin, Y. Du, C. Wang, and B. Jia, "Ultra-long-distance interferometric DOFS over 300 km without in-line repeater," *IEEE Photon. Technol. Lett.*, vol. 37, no. 5, pp. 289–292, Mar. 1, 2025.

[9] Q. Chen et al., "A distributed fiber vibration sensor utilizing dispersion induced walk-off effect in a unidirectional Mach–Zehnder interferometer," *Opt. Exp.*, vol. 22, no. 3, pp. 2167–2173, Feb. 2014.

[10] J. Huang et al., "A 150 km distributed fiber-optic disturbance location sensor with no relay based on the dual-Sagnac interferometer employing time delay estimation," *Opt. Commun.*, vol. 479, Jan. 2021, Art. no. 126420.

[11] Y. Yan, F. N. Khan, B. Zhou, A. P. T. Lau, C. Lu, and C. Guo, "Forward transmission based ultra-long distributed vibration sensing with wide frequency response," *J. Lightw. Technol.*, vol. 39, no. 7, pp. 2241–2249, Apr. 1, 2021.

[12] Y. Yan, H. Zheng, A. P. T. Lau, C. Guo, and C. Lu, "Unidirectional ultra-long distributed optical fiber sensor," *IEEE Photon. J.*, vol. 13, no. 4, pp. 1–7, Aug. 2021.

[13] B. J. Puttnam, G. Rademacher, and R. S. Luís, "Space-division multiplexing for optical fiber communications," *Optica*, vol. 8, no. 9, pp. 1186–1198, 2021.

[14] Z. Zhao, L. Shen, Y. Dang, C. Lu, and M. Tang, "Enabling long range distributed vibration sensing using multicore fiber interferometers," *Opt. Lett.*, vol. 46, no. 15, pp. 3685–3688, Aug. 2021.
[15] G. Yin, Z. Xu, J. Ma, and T. Zhu, "Simultaneous measurement of bending and torsion in optical fiber shape sensor," *J. Lightw. Technol.*, vol. 41, no. 6, pp. 1851–1857, Mar. 2023.
[16] Y. Zhang, Z. Fang, and G. Zhou, "A stable and highly sensitive directional torsion sensor based on a helical double cladding microstructured multicore fiber," *IEEE Sensors J.*, vol. 24, no. 5, pp. 6166–6172, Mar. 2024.
[17] S. Chen, Y. Ma, C. Jiang, C. Mou, and Y. Liu, "Characteristics of helical long-period gratings inscribed in seven-core fibers by CO_2 laser," *J. Lightw. Technol.*, vol. 42, no. 10, pp. 3826–3834, May 15, 2024.
[18] X. Luo, D. Zheng, S. Chen, Y. Liu, and W. Peng, "Liquid-filled multicore elastic optical waveguide for multi-point bending sensing," *IEEE Photon. Technol. Lett.*, vol. 37, no. 15, pp. 817–820, Aug. 1, 2025.
[19] Y. Zhao, H. Peng, Y. Ma, Y. Liu, Y. Yang, and Z. He, "Helical long-period gratings in four-core fiber for multiparametric monitoring of directional bending, torsion and temperature," *J. Lightw. Technol.*, vol. 41, no. 13, pp. 4437–4443, Jul. 1, 2023.
[20] M. Cui, Z. Wang, and C. Yu, "Refractive index sensing using helical broken-circular-symmetry core microstructured optical fiber," *Sensors*, vol. 22, no. 23, p. 9523, Dec. 2022.
[21] Y. Dai, M. Yang, G. Xu, and Y. Yuan, "Magnetic field sensor based on fiber Bragg grating with a spiral microgroove ablated by femtosecond laser," *Opt. Exp.*, vol. 21, no. 14, pp. 17386–17391, 2013.
[22] R. Beravat, G. K. L. Wong, X. M. Xi, M. H. Frosz, and P. St. J. Russell, "Current sensing using circularly birefringent twisted solid-core photonic crystal fiber," *Opt. Lett.*, vol. 41, no. 7, pp. 1672–1675, Apr. 2016.
[23] Z. Wang et al., "Coherent Φ-OTDR based on I/Q demodulation and homodyne detection," *Opt. Exp.*, vol. 24, no. 2, pp. 853–858, 2016.
[24] G. Y. Chen et al., "Long-range distributed vibration sensing using phase-sensitive forward optical transmission," *Opt. Lett.*, vol. 48, no. 18, pp. 4825–4828, Sep. 2023.
[25] X. Rao et al., "Multi-point vibration positioning method for long-distance forward transmission distributed vibration sensing," *Opt. Exp.*, vol. 32, no. 17, pp. 30775–30786, Aug. 2024.

Danxia Lu was born in Guangdong, China, in 2001. She received the B.S. degree in light sources and lighting from Guangdong Polytechnic Normal University, Guangzhou, China, in 2023. She is currently pursuing the M.S. degree with Shenzhen University, Shenzhen, China.

Her research interests include SDM distributed multiparameter sensing based on phase-sensitive forward transmission of light.

Xing Rao was born in Jiangxi, China, in 1998. He received the B.S. degree in optoelectronic information science and engineering from Nanchang Hangkong University, Nanchang, China, in 2020, and the Ph.D. degree from Shenzhen University, Shenzhen, China, in 2025.

He is currently a Postdoctoral Researcher at Shenzhen University. His current research interests focus on integrated sensing and communication.

Shangwei Dai was born in Guangxi Zhuang Autonomous Region, China, in 1998. He received the master's degree in electronic information from Shantou University, Shantou, China, in 2023. He is pursuing the Ph.D. degree with Shenzhen University, Shenzhen, China.

His current research interests focus on super-long-range distributed vibration sensors based on phase-sensitive forward transmission of light.

Shen Liu is a Deputy Director of Shenzhen Key Laboratory of Photonic Devices and Sensing Systems for Internet of Things, selected as one of Shenzhen's outstanding scientific and technological innovation talents, Shenzhen's overseas high-level talents, top 2% of the world's top scientists in the "Scientific Influence Ranking," and Shenzhen University's, Shenzhen, China, "Li-Yuan Excellent Young Scientists," etc. Research directions include fiber-optic sensing technology, extreme environment mechanics sensing technology, fiber-optic microcavity gas sensing technology, inertial devices, and system applications; around the aerospace force thermal in situ measurements and air and space inertial navigation core devices, to carry out fiber-optic microcavity resonance device fabrication technology, sensing applications, system integration, and other research.

Dr. Liu has been awarded with the Nomination Prize of the National Outstanding Doctoral Dissertation of Optical Engineering, the Second Prize of the Ministry of Education's Natural Science Prize, and the First Prize of the Optics Science and Technology Prize of the Optical Society of Guangdong Province.

Guo-Wei Lu (Member, IEEE), photograph and biography not available at the time of publication.

Yiping Wang (Senior Member, IEEE) was born in Chongqing, China, in 1971. He received the B.Eng. degree in precision instrument engineering from Xi'an Institute of Technology, Xi'an, China, in 1995, and the M.S. and Ph.D. degrees in optical engineering from Chongqing University, Chongqing, China, in 2000 and 2003, respectively.

From 2003 to 2005, he was with Shanghai Jiao Tong University, Shanghai, China, as a Postdoctoral Fellow. From 2005 to 2007, he was with Hong Kong Polytechnic University, Hong Kong, as a Postdoctoral Fellow. From 2007 to 2009, he was with the Institute of Photonic Technology (IPHT), Jena, Germany, as a Humboldt Research Fellow. From 2009 to 2011, he was with the Optoelectronics Research Center (ORC), University of Southampton, Southampton, U.K., as a Marie Curie Fellow. Since 2012, he has been with Shenzhen University, Shenzhen, China, as a Distinguished Professor. He has authored or co-authored one book, 53 invention patents, and more than 420 journal articles and conference papers. His current research interests focus on optical fiber sensors, fiber gratings, and photonic crystal fibers.

Prof. Wang is a Fellow of Optica and Chinese Optical Society.

George Y. Chen (Senior Member, IEEE) received the M.Eng. degree (bachelor's and master's joint degrees) in the field of electronics and electrical engineering with computer science from Imperial College London, London, U.K., in 2009, and the Ph.D. degree from the Optoelectronics Research Center, University of Southampton, Southampton, U.K., in 2014.

From 2013 to 2015, he was a Postdoctoral Research Fellow for SPI Lasers Ltd., Southampton, with the Industrial Research Laboratory. In 2015, he joined the University of South Australia, Adelaide, SA, Australia, as a Research Fellow and a Senior Research Fellow in 2019. He was a part of the MinEx CRC, Perth, WA, Australia. In 2021, he joined Shenzhen University, Shenzhen, China, as a Professor.

Dr. Chen is a Senior Member of Optica.